11-1995

Analysis of Ladar Range Resolution Enhancement by Sinusoidal Phase Modulation

Leonard T. Masters
Consultant

Martin B. Mark
U.S. Air Force Academy

Bradley D. Duncan
University of Dayton, bduncan1@udayton.edu

Analysis of ladar range resolution enhancement by sinusoidal phase modulation

Leonard T. Masters
University of Dayton
Center for Electro-Optics
300 College Park
Dayton, Ohio 45469-0226

Martin B. Mark, MEMBER SPIE
Wright Laboratory
AARI-2, Electro-Optics Sensors Group
Wright Patterson Air Force Base, Ohio 45433

Bradley D. Duncan, MEMBER SPIE
University of Dayton
Center for Electro-Optics
300 College Park
Dayton, Ohio 45469-0226

Abstract. The ability of a ladar system to resolve two or more separate returns from a combined echo is related to the effective correlation bandwidth of the pulse emitted by the ladar system. Phase modulation of an outgoing pulse introduces additional frequency components, which increases the effective correlation bandwidth of the pulse and thus improves the range resolution of the system. In this paper, we discuss the general theoretical basis for achieving improved range resolution using a modulated waveform and a matched filter receiver. We then demonstrate these concepts by considering the particular case of improved range resolution for a sinusoidally phase modulated carrier with a rectangular amplitude function. We also perform computer simulations with a realistic pulsed ladar envelope possessing the same modulation function. Our calculations indicate that the resolution of a pulsed ladar system may be improved by a factor of 70 with a phase-modulated pulse and a matched-filter receiver.

Subject terms: optical remote sensing and image processing; ladar; phase modulation; pulse compression; matched filtering; ambiguity function; range resolution.

Optical Engineering 34(11), 3115–3121 (November 1995).

1 Introduction

Ladar (laser detection and ranging) constitutes a direct extension of conventional radar techniques to very short wavelengths.[1] The shift in wavelength provides increased accuracy and improved resolution in delay (range) as well as Doppler (velocity) measurements. Although fairly new, ladar has already found many applications within industry and the military. These applications include range finding[2,3] and range-velocity imaging.[4,5] Because radar and ladar differ only in wavelength, the proven modulation techniques of radar may be applied to laser transmitters to improve target parameter estimation. However, ladar has been slow to adopt these modulation techniques (called pulse compression techniques), due to the technological difficulties of impressing arbitrary waveforms on an optical carrier. As the technology has matured, though, optical modulators have improved,[6,7] and the investigation of modulated ladar pulses has followed suit.[8]

For our work here, the parameter we are interested in improving is the range resolution of the ladar system. Range resolution is the minimum separation between targets such that they can be resolved as separate and distinct by the ladar system. With simple, unmodulated pulsed waveforms (those waveforms with a time-bandwidth product on the order of unity), range resolution is directly related to pulse duration, while velocity resolution is inversely related to pulse duration. That is, as the pulse duration decreases, the range resolution also decreases (improves), and the velocity resolution increases (degrades). Of course, if the pulse duration is increased, then the converse is true.

Obviously, the desired range resolution improvement may be achieved by decreasing the temporal duration of the transmitted pulse. However, since detection and accuracy are dependent on the signal energy, the transmitted peak power must be raised in proportion to the reduction in pulse duration. Also, there is an additional difficulty if the target's velocity is to be measured, as the sensitivity of a signal to the range rate depends on the duration of the coherently processed signal. Due to these constraints, long pulses are often desirable and another technique must be found for improving the range resolution.

P. M. Woodward has demonstrated that range resolution is actually related to pulse bandwidth, not pulse duration.[9] That is, it is possible to achieve the same resolution with a modulated, long-duration pulse as with an unmodulated, short-duration pulse. Such improvements in resolution with long-duration pulses may be achieved using a technique, first developed in the field of radar, called pulse compression. As implied by the name, the objective is to compress the received signal to allow recognition of closely spaced objects.[10] In

Paper RS-002 received Apr. 10, 1995; revised manuscript received June 1, 1995; accepted for publication June 19, 1995.

fact, pulse compression waveforms have been used to increase time-bandwidth products and are known for allowing accurate, simultaneous estimates of range and velocity.

In part, pulse compression is implemented by using a matched or correlation receiver. That is, the receiver's impulse response has the same shape as the transmitted signal, except for a reversal of the time axis. Thus the receiver can be said to be "matched" to the transmitted waveform. One of the advantages of using this type of receiver is that matched filter receivers are designed for optimum signal detection in the presence of stationary white Gaussian noise.[10]

Our proposed method for experimentally implementing pulse compression and matched filtering is discussed in Sec. 2. In Sec. 3, we present the theoretical basis for target resolution, and in Sec. 4 we discuss sinusoidal phase modulation. The results of Secs. 3 and 4 are then implemented in Sec. 5 to derive an expression for range resolution as a function of modulation index for a rectangular amplitude ladar pulse. In Sec. 6, we present computer simulations to illustrate theoretical improvements in the range resolution for a realistic ladar amplitude function. Our conclusions are discussed in Sec. 7.

2 The Heterodyne Ladar Transceiver

Figure 1 is a diagram of a monostatic ladar system that we have used for previous ladar experiments.[11] The master oscillator (MO), made by CLR Photonics,[12] emits an eyesafe ($\lambda = 2.09$ μm) monochromatic, continuous-wave Gaussian beam, a portion of which is split off at the first beamsplitter (BS-1), and directed toward the detection electronics. This portion of the MO output will later serve as the reference beam for heterodyne detection. The rest of the MO output then propagates through a NEOS[13] acousto-optic modulator, which upshifts the exiting radiation's frequency by 27 MHz. Next, the upshifted MO beam is directed into a CTI[14] slave oscillator cavity, where it serves as an injection seed to lock the slave oscillator's more powerful, pulsed output to the narrowband frequency of the MO output. Linearly polarized slave-oscillator output then exits through the output coupler and propagates through a ConOptics[15] electro-optic crystal. This electro-optic crystal and the resonant circuit that drives it form the phase modulator. After passing through the phase modulator, the now sinusoidally modulated ladar pulse propagates to a transmit-receive switch consisting of a Brewster-angle thin-film polarizer and a quarterwave plate. As the degree of reflectance of the Brewster-angle polarizer is dependent on the incident angle, the angle of incidence is set so the majority of the transmit pulse is directed outward toward a target through the quarterwave plate. A small portion of the output, however, is allowed to pass through the polarizer. This throughput pulse is reflected through a second beamsplitter (BS-2) and is mixed with the reference beam. The mixed beam is then detected and recorded by a digitizing oscilloscope. This waveform will serve as the matched filter for the return signal.

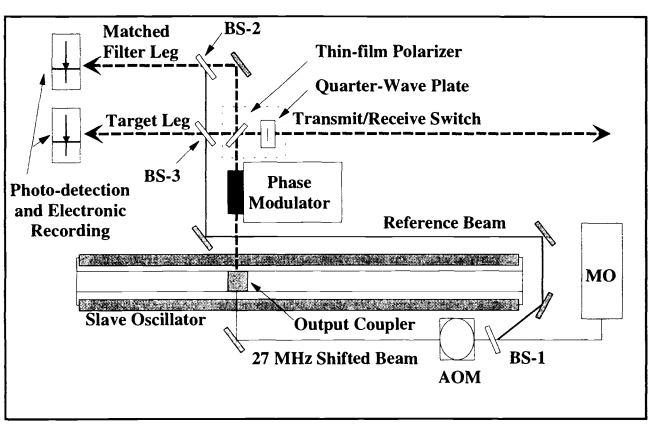

Fig. 1 Schematic illustration of the proposed ladar system.

The portion of the modulated pulse that is reflected by the Brewster-angle polarizer propagates through the quarterwave plate before exiting the system. Thus the linear polarization of the slave output is converted to circular polarization before it is transmitted to the target. After reflecting off the target, the return pulse remains primarily circularly polarized, but with opposite handedness to the transmitted pulse. When the return pulse propagates back through the ladar system, it passes through the quarterwave plate again. On this second pass, the circular polarization of the return pulse is changed back to linear polarization. However, the opposite handedness of the ladar return pulse forces the direction of polarization to be orthogonal to that of the transmitted pulse. The return pulse thus passes through the transmit-receive switch and propagates through the third beamsplitter (BS-3), where it mixes with the reference beam. After detection, the intermediate-frequency signal at 27 MHz is recorded by a digitizing oscilloscope. Matched filter output is then obtained by correlating the recorded return pulse and its matched filter response.

3 Comparative Signal Analysis

The pulse transmitted by the ladar system in Fig. 1 may be represented by

$$s(t) = a(t)\ \cos[\omega_c t + \phi(t)]\ , \tag{1}$$

where $a(t)$ is an amplitude function, $\phi(t)$ represents a general phase function, and ω_c is the carrier frequency. The analysis to follow, however, becomes much easier if the general ladar pulse given in Eq. (1) is represented using complex phasor notation, such that $s(t)$ is expressed by the following equation:

$$s(t) = \mathrm{Re}\{\psi(t)\} = \mathrm{Re}\{\mu(t)\ \exp(j\omega_c t)\}\ , \tag{2}$$

where the phasor (complex envelope function) $\mu(t)$ is given by

$$\mu(t) = a(t)\ \exp[j\phi(t)]\ . \tag{3}$$

The complex envelope function is shown below to represent the most important portion of the pulse for improving range resolution.

A return signal from two objects (of equal reflectivity) can now be defined and is given by

$$\psi_r(t) = \psi(t - t_0) + \psi(t - t_0 - \tau)\ , \tag{4}$$

where t_0 is the round-trip delay for the first target, and τ is the difference in delay between the two targets. Note that we may take t_0 to be zero without loss of generality. Now to

resolve two closely spaced objects we would like the echoes from them to appear as dissimilar as possible.[16] For our work, we take the measure of dissimilarity between the two signals to be the integrated squared magnitude of the difference[10] as given in the following equation:

$$\varepsilon^2 = \int_{-\infty}^{\infty} |\psi(t) - \psi(t-\tau)|^2 \, dt \ . \tag{5}$$

This quantity will not only provide a general feel for the desirable properties of the complex envelope function $\mu(t)$, but will also be used in the derivation of the predicted range resolution. Expanding the squared term in Eq. (5), we obtain

$$\varepsilon^2 = \int_{-\infty}^{\infty} |\psi(t)|^2 \, dt + \int_{-\infty}^{\infty} |\psi(t-\tau)|^2 \, dt - \int_{-\infty}^{\infty} \psi(t)\psi^*(t-\tau) + \psi^*(t)\psi(t-\tau) \, dt \ . \tag{6}$$

Note that the first two integrals of Eq. (6) are equivalent, one being simply a temporally shifted version of the other. Also note that the carrier term embedded within Eq. (6) only shifts the spectrum of the pulse and has no effect on ε^2. Simplifying Eq. (6) and ignoring the carrier term, we find

$$\varepsilon^2 = 2\int_{-\infty}^{\infty} |\mu(t)|^2 \, dt - 2 \ \mathrm{Re}\left\{ \int_{-\infty}^{\infty} \mu^*(t)\mu(t-\tau) \, dt \right\} \ . \tag{7}$$

In Eq. (7) the first term on the right-hand side is twice the energy contained in the pulse and is presumed constant. The second integral, though, is recognized as the autocorrelation of the complex envelope function. This implies that the ladar pulse waveform should be chosen so that its autocorrelation is as near zero as possible, except when $\tau = 0$, where it is by definition a maximum. We also note that in the context of range resolution theory, the complex envelope's autocorrelation is defined as the *range ambiguity function*[17] $c_\mu(t)$, given as

$$c_\mu(\tau) = \int_{-\infty}^{\infty} \mu(t)\mu^*(t-\tau) \, dt \ . \tag{8}$$

Recall that the autocorrelation function is a measure of how similar a function is to its shifted version. If a signal looks the same throughout its duration, the autocorrelation will be broad. Conversely, the autocorrelation, and thus the range ambiguity function, will be narrow if any given portion of the signal is dissimilar to all other parts. Now, the ideal delta-function matched-filter output is physically unrealizable, and generally the range ambiguity function (i.e., autocorrelation function) will have significant magnitude at values of τ away from the main lobe. Where this is true, there are range sidelobes. As we show in Sec. 6, these sidelobes may produce "ghost images" that may mask another target and lead to ambiguities, which futher complicate the target resolution process.

Burdic takes the comparative signal analysis further by using the integrated squared difference ε^2 to compare the spectrum of the autocorrelation of the transmitted pulse with the spectrum of an impulse function. By comparing the two spectra, Burdic arrives at a quantity defined as the effective correlation bandwidth β_e, given by

$$\beta_e = \frac{c_\mu^2(0)}{\int_{-\infty}^{\infty} |c_\mu(t)|^2 \, dt} \ . \tag{9}$$

The effective correlation bandwidth implies a certain range resolution capability for the signal. The larger the effective correlation bandwidth, the more "impulselike" is the autocorrelation function, and therefore the better the inherent range resolution of the signal.[10]

The minimum separation in range between two targets—the range resolution δr—may be found by dividing the speed of light by twice the effective bandwidth,[17] where the factor of two takes into account the propagation through twice the line-of-sight distance from ladar system to object and back. Thus the range resolution is given by

$$\delta r = \frac{c}{2\beta_e} = \frac{c}{2c_\mu^2(0)} \int_{-\infty}^{\infty} |c_\mu|^2 \, d\tau \ . \tag{10}$$

We note that the range resolution of the system is directly related to the area under the square magnitude of the complex envelope's autocorrelation function. Thus, improved resolution implies a complex envelope function that has little area under its autocorrelation function. Equation (10) and the results of Sec. 4 are used below to derive an expression for range resolution as a function of modulation index.

4 Sinusoidal Phase Modulation

Electro-optic modulators have improved in recent years; however, impressing arbitrary phase modulation waveforms onto an optical carrier at longer eyesafe wavelengths is still difficult. Simple phase modulation functions, however, are easier to implement. For our work, we have chosen the simplest waveform, i.e., a sinusoid. By placing the electro-optic crystal in a resonant circuit, the sinusoidal phase modulation function is impressed on the carrier by simply driving the circuit with a signal generator set at the appropriate modulation frequency.

An electro-optic crystal such as lithium niobate ($LiNbO_3$) changes the phase of an electromagnetic wave as a changing voltage is applied across the crystal. Specifically, an applied potential induces a phase change $\Delta\varphi$ in an optical wave passing through the crystal according to[18]

$$\Delta\varphi = \frac{\pi}{\lambda} n_e^3 r \frac{l}{d} V \ , \tag{11}$$

where λ is the optical wavelength, n_e is the extraordinary index of refraction, r is the linear susceptibility coefficient, l is the length of the crystal, d is the crystal thickness, and V is the applied voltage.

So that we may use off-the-shelf components, we place the modulator in a high-Q resonant LC circuit. The center frequency of an LC resonant circuit is determined by the inductance and capacitance according to

$$\omega_m = \frac{1}{\sqrt{LC}} \ , \tag{12}$$

where ω_m is the center frequency of the resonant circuit, L is the inductance, and C, in our case, is the capacitance of the electro-optic crystal. Also, the potential across the capacitor in the resonant circuit is the voltage applied to the resonant circuit multiplied by the quality factor Q of the resonant circuit.[19] Therefore, with a high-Q resonant circuit, a small input voltage from a standard waveform generator will translate into a larger voltage across the electro-optic crystal, and thus a relatively large peak phase deviation.

One of the important characteristics of a modulated waveform is its spectrum. For sinusoidal phase modulation, we substitute into Eq. (3) the phase function

$$\phi(t)=\beta\ \sin\omega_m t\ , \tag{13}$$

where β is the modulation index. In the case of phase modulation, the modulation index is simply equal to the peak phase deviation. Note that $\phi(t)$ is periodic, and thus so is $\mu(t)$. Using a Fourier series expansion, we find that the spectrum of the sinusoidally phase modulated carrier signal is a summation of sinusoids with amplitudes given by Bessel functions of the first kind.[20] Thus, the complex envelope can be represented as

$$\mu(t)=a(t)\ \exp(j\beta\ \sin\omega_m t)=a(t)\sum_{n=-\infty}^{\infty} J_n(\beta)\ \exp(jn\omega_m t)\ . \tag{14}$$

This alternative representation of the complex envelope and the expression for range resolution presented earlier in Sec. 3 are used in the following section to illustrate how a modulated waveform may improve the ladar system range resolution.

5 Rectangular-Waveform Performance

To demonstrate the general concept of increased range resolution due to carrier phase modulation, we present the closed-form solution for a waveform with a simple amplitude function. Specifically, we take the amplitude function $a(t)$ to be a unit-amplitude rectangle function

$$a(t)=\mathrm{rect}\left(\frac{t}{t_p}\right)=\begin{cases}1, & -t_p/2\leq t\leq t_p/2\ ,\\ 0, & |t|>t_p/2\ ,\end{cases} \tag{15}$$

where t_p is the pulse duration. To correspond with a real pulse emitted by the system in Fig. 1, this pulse duration is set at 500 ns. We also take the modulation function to be the sinusoidal function given in Eq. (13). To determine the range solution, we now start by finding the autocorrelation of the complex envelope function. Thus, inserting Eqs. (14) and (15) into Eq. (8), we find

$$c_\mu(\tau)=\int_{-\infty}^{\infty}\mathrm{rect}\left(\frac{t}{t_p}\right)\mathrm{rect}\left(\frac{t-\tau}{t_p}\right)\sum_{n=-\infty}^{\infty}\sum_{m=-\infty}^{\infty}J_n(\beta)$$
$$\times\exp(jn\omega_m t)\ J_m(\beta)\ \exp[-jm\omega_m(t-\tau)]\ \mathrm{d}\tau\ . \tag{16}$$

After performing the integration and simplifying, the range ambiguity function becomes

$$c_\mu(\tau)=\sum_n\sum_m J_n(\beta)J_m(\beta)\ \exp\left[\ j(n+m)\frac{\omega_m}{2}\tau\ \right]\ (t_p-|\tau|)$$
$$\times\mathrm{Sa}\left\{(n-m)\frac{\omega_m}{2}(t_p-|\tau|)\right\}\ , \tag{17}$$

where the function Sa is defined as the sine-over-argument function.[20] Notice also that evaluating Eq. (17) at $\tau=0$ gives the denominator of Eq. (10) and yields

$$c_\mu(0)=t_p\ . \tag{18}$$

Now, if we substitute Eqs. (17) and (18) into Eq. (10), we find the range resolution δr for sinusoidally modulated rectangular pulse to be

$$\delta r=\frac{c}{2t_p^2}\int_{-t_p}^{t_p}\left|\sum_n\sum_m J_n(\beta)J_m(\beta)\ \exp[j(n+m)\frac{\omega_m}{2}\tau](t_p-|\tau|)\right.$$
$$\left.\times\mathrm{Sa}\left\{(n-m)\frac{\omega_m}{2}(t_p-|\tau|)\right\}\right|^2\mathrm{d}\tau\ . \tag{19}$$

In Fig. 2, δr is plotted versus the modulation index for three different modulation frequencies. Note that as the modulation frequency is increased, an improvement in range resolution for a given modulation index is achieved. However, it is a modest gain and must be weighed against the resulting ambiguities. As we will see in Sec. 6, the larger modulation frequencies produce range ambiguity functions that have several significant secondary maxima as discussed in Sec. 3. These secondary maxima, or range sidelobes, are caused by the modulation frequency going through multiple cycles over the duration of the pulse envelope. The range sidelobes appear when the pulse's temporal duration exceeds the modulation period. In addition, as the modulation frequency is increased beyond that point, more range sidelobes appear, and they increase in magnitude. As a result, range sidelobes contribute more area to the autocorrelation function, and degrade the range resolution. This can be seen in Fig. 2 on comparing the range resolution improvement as the modulation frequency is increased. We see that there is a greater improvement in range resolution on increasing the modulation frequency from 2 to 4 MHz than there is on increasing it from 4 to 8 MHz. In fact, after a point there is no significant improvement at all, while the range sidelobes will have greatly increased the range ambiguities. From Fig. 2, it is clearly better to attempt enhanced range resolution by increasing the modulation index rather than by increasing the modulation frequency.

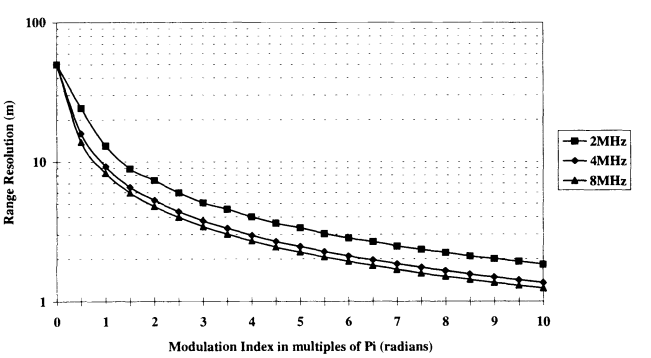

Fig. 2 Range resolution versus modulation index for three different modulation frequencies with a rectangular envelope.

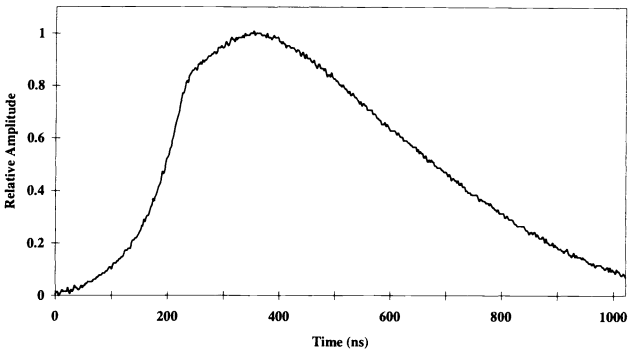

Fig. 3 Ladar pulse from slave oscillator: transmitted pulse from the ladar system shown in Fig. 1.

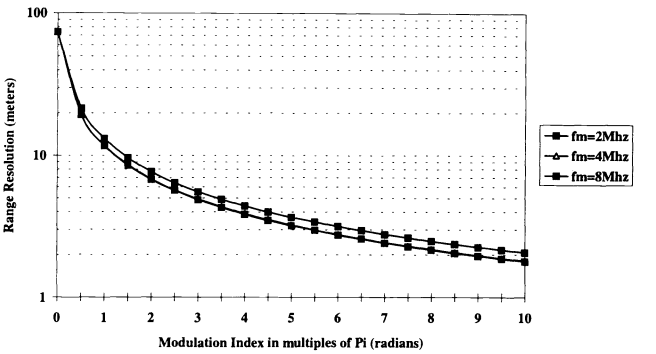

Fig. 4 Range resolution versus modulation index: the range ambiguity function for a realistic pulsed-ladar envelope function. The modulation frequency is 3 MHz; for $\beta = 15\pi$ the range resolution is approximately 1 m.

6 Computer Simulations with a Real Ladar Envelope

The following simulations were performed using the DADiSP® software package. Due to the complicated nature of the amplitude function for a real ladar pulse envelope, an analytical form for range resolution was not derived. Instead, range resolution was calculated by numerically implementing Eq. (10) using the complex envelope function given in Eq. (14), with the amplitude function $a(t)$ as shown in Fig. 3. The pulse in Fig. 3 has a FWHM duration of 500 ns, and is generated by the slave oscillator shown in Fig. 1. Again, we calculated the range resolution as a function of modulation index for three different frequencies. As can be seen in Fig. 4, an unmodulated pulse ($\beta = 0$) has a range resolution of approximately 70 m. Figure 4 also illustrates that increasing the modulation frequency has even less of an effect on improving range resolution, for a given modulation index, when the amplitude function is more realistic. In fact, there is no improvement achieved by increasing the modulation frequency from 4 to 8 MHz.

Several suppliers of electro-optic modulators were polled to find a realistic value for the highest achievable modulation index. ConOptics[15] quoted a reasonable estimate of 15π. Using this value for the modulation index and choosing a modulation frequency of 3 MHz, we determined the range ambiguity function and calculated the range resolution for the more realistic ladar envelope function. A range resolution of approximately 1 m was calculated for the modulated waveform, which represents a factor-of-70 improvement. We note that the modulation frequency of 3 MHz was chosen as a compromise between ambiguous sidelobes and improved range resolution.

Although these results are encouraging, a modulation index of 15π is presently beyond what is achievable with our available equipment. With our available equipment, a maximum modulation index of 2π is possible. Performing the calculation with this modulation index and a modulation frequency of 3 MHz, we find the range resolution is substantially larger—approximately 6 m. Note that a difference in range of 6 m corresponds to two targets separated by a delay of 40 ns.

Figure 5 shows a simulated waveform immersed in white noise. The waveform consists of a composite return pulse for two targets of equal reflectivity separated in delay by 40 ns. We adjusted the amount of added white noise to correspond to a signal-to-noise ratio of approximately 5 dB. This signal-to-noise ratio was chosen to be near the minimum where the signal could be said to be reliably detected.[21] Figure 6 shows the matched filter output for the simulated noisy waveform. The matched filter output clearly indicates the presence of two targets; however, the absolute locations in delay are off slightly. This is because the smaller range sidelobes surrounding the main lobe affect the absolute positions predicted by the matched filter. However, resolution of the two targets is still achieved even in the presence of strong noise.

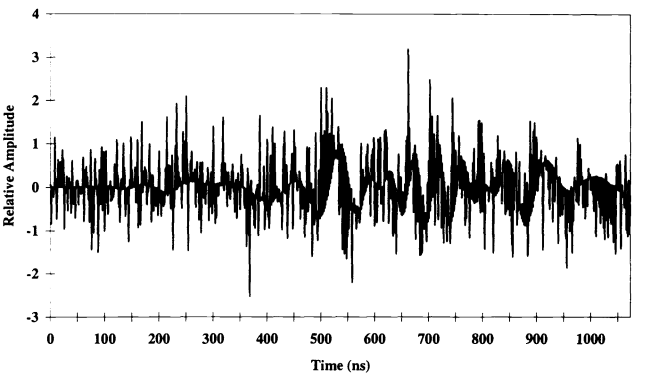

Fig. 5 Combined heterodyned return signal consisting of echoes from two targets of equal ladar cross section, with white noise added.

Recall that as the modulation frequency is increased, we have claimed that the range resolution improves only modestly for a given modulation index. This is due to the presence of several significant sidelobes in the ambiguity function. In addition to increasing the area under the ambiguity function, thereby degrading the range resolution, these sidelobes may result in ghost images as illustrated in Fig. 7. The ambiguity function in Fig. 7 was produced by a waveform modulated at 12 MHz with a modulation index of 15π. Even though the range resolution was calculated to be about 0.9 m, the large sidelobes introduce intolerable range ambiguities. That is, the range sidelobes make it appear as though there were other targets present (i.e., ghost images) spaced by approximately 90 ns in delay.

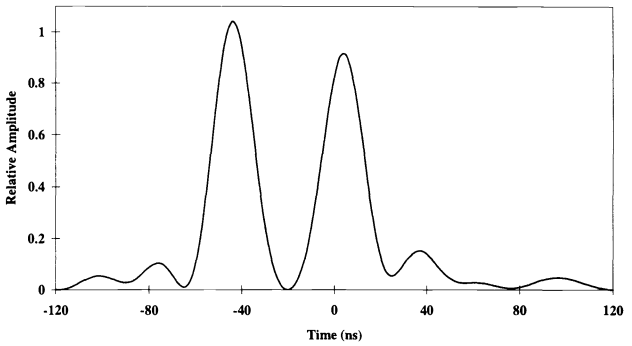

Fig. 6 Matched filter output for two targets: This range ambiguity function shows two distinct peaks near the time delays of the targets, even in the presence of strong noise.

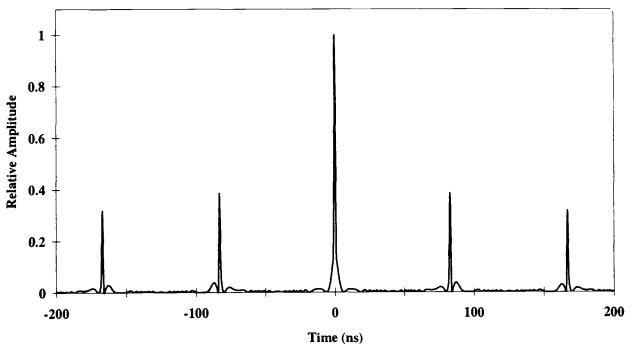

Fig. 7 Matched filter output (large f_m and β): This ambiguity function demonstrates that even though the calculated range resolution is small (approximately 1 m), the significant range sidelobes introduce unacceptable ambiguities when the modulation frequency and modulation index are high.

Table 1 The known Barker sequences that are used in discrete phase coding.

Code Length	Code Elements
1	+
2	+ -, + +
3	+ + -, + - +
4	+ + - +, + + + -
5	+ + + - +
7	+ + + - - + -
11	+ + + - - - + - - + -
13	+ + + + + - - + + - + - +

Since the effective correlation bandwidth increases with a phase function that is nonlinear, a more highly nonlinear technique can reduce the area under the ambiguity function by driving down the range sidelobes. This will allow for improved range resolution at high modulation frequencies, without the difficulties introduced by ghost images. One such optimum form of discrete phase coding is implemented using Barker codes[22] or Barker sequences. All known Barker codes are shown in Table 1, where a + represents no phase change in the carrier, while a − represents a phase shift of π rad.

Barker-sequence encoding may be accomplished by placing a second phase modulator after the first one in Fig. 1.

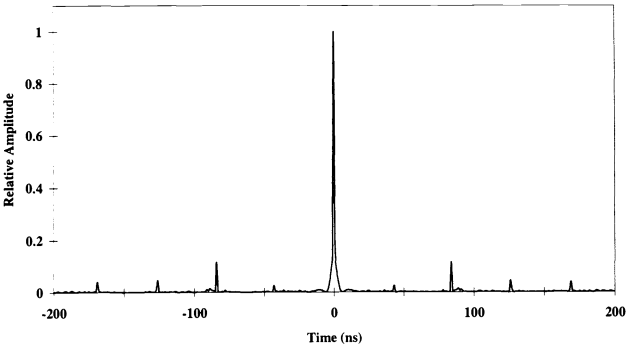

Fig. 8 Matched filter output (mixed modulation): This ambiguity function illustrates the effect an 11-bit Barker code has on reducing range sidelobes.

This second modulator would then be turned either on or off, depending on the value of the phase shift. The only requirement is that the second modulator has to be synchronized with the transmitted pulse, while the first is allowed to run continuously.

In Fig. 8, the matched-filter output from a waveform with mixed modulation (both sinusoidal and discrete phase coding) is shown. As in Fig. 7, the modulation frequency and the modulation index are 12 MHz and 15π, respectively; the only difference is that an 11-bit Barker code has been added to the sinusoidal phase modulation. From this diagram the theoretical range resolution was found to be approximately 0.4 m, and it is clear that the range sidelobes have been significantly reduced. Clearly, the Barker-code technique is an additional method of improving the range resolution capability of a pulsed ladar system.

7 Summary

Herein we have discussed a technique for extending the pulse compression methods of conventional microwave radar to the ladar regime. We have presented the theoretical background of enhanced range resolution and demonstrated that the resolution of a pulse is proportional to the effective correlation bandwidth and not the pulse's temporal duration. Furthermore, we have studied a method for phase modulation by utilizing an electro-optic modulator inside a resonant circuit. Initial simulations have been performed and support the hypothesis that range resolution can be appreciably improved simply by the implementation of sinusoidal phase modulation and matched filtering.

The results of our analysis are encouraging. By placing an electro-optic crystal in the beam path and driving it with a simple resonant circuit, it is possible to increase the range resolution by a factor of 70. Another advantage is that on simply turning off the driving circuit the modulator only introduces a fixed phase and in effect becomes transparent to the system. In this way it is possible to take full advantage of the velocity resolution capability inherent in a long-pulse ladar system without changing the geometry of the system. Thus the system can be made to operate at either optimum range resolution, optimum velocity resolution, or combined range and velocity resolution modes by controlling the driving circuit. Our continuing efforts will center on incorporating this enhancement technique into our existing ladar system.

Acknowledgments

The authors would like to thank the Wright Laboratory Electro-Optic Sensor Group as well as the University of Dayton Center for Electro-Optics. This work has been sponsored by the Wright Laboratory Avionics Directorate and Technology/Scientific Services Inc. of Dayton Ohio, under contract F33601-95-DJ010.

References

1. A. V. Jelalian, *Laser Radar Systems,* Artech House, Boston, MA (1992).
2. J. Kostamovaara, K. Maatta, and M. Koskinen, "Pulsed laser radars with high-modulation frequency in industrial applications," in *Laser Radar VII, Proc. SPIE* **1633,** 114–127 (1992).
3. J. H. Woodward, *The AN/GVS-5 Hand Held Laser Range Finder,* RCA Electro-Optics, Moorestown, NJ, pp. 76–79 (1977).
4. A. L. Kachelmyer, "Range-Doppler imaging: waveforms and receiver design," in *Lasar Radar III, Proc. SPIE* **999,** 138–161 (1988).
5. A. L. Kachelmyer, "Range Doppler imaging with a laser radar," *Lincoln Lab. J.* **3**(1), 87–118 (1990).
6. B. Lax, "Theory of single and double sideband modulators," in *Lasar Radar VII, Proc. SPIE* **1633,** 206–215 (1992).
7. N. W. Harris, J. M. Sobolewski, C. L. Summers, and R. S. Eng, "The design and construction of a wideband efficient electro-optic modulator," in *Laser Radar VI, Proc. SPIE* **1416,** 59–69 (1991).
8. R. S. Eng, N. W. Harris, and C. L. Summers, "Tunable electro-optic modulators for laser radar applications—experimental results," in *Laser Radar VII, Proc. SPIE* **1633,** 216–227 (1992).
9. P. M. Woodward, *Probability and Information Theory with Applications to Radar,* McGraw-Hill, New York (1953).
10. A. W. Rihaczek, *Principles of High-Resolution Radar,* McGraw-Hill, New York (1969).
11. J. A. Overbeck, M. B. Mark, S. H. McCracken, P. F. McManamon, and B. D. Duncan, "Coherent versus incoherent ladar detection at 2.09 μm," *Opt. Eng.* **32**(11), 2681–2689 (Nov. 1993).
12. CLR Photonics Inc., Boulder, CO 80306, (303) 449-8736.
13. NEOS Technologies Inc., Melbourne, FL 32904, (407) 676-9020.
14. Coherent Technologies Inc., Boulder, CO 80306, (303) 449-8736.
15. Conoptics Inc., Eagle Road, Danbury, CT 06810, (203) 742-3349.
16. W. S. Burdic, *Radar Signal Analysis,* Prentice-Hall, London (1968).
17. H. Urkowitz, in *Modern Radar, Analysis, Evaluation, and System Design,* R. S. Berkowitz, Ed., Wiley, New York (1979).
18. A. Yariv and P. Yeh, *Optical Waves in Crystals,* Wiley, New York (1984).
19. J. W. Nilsson, *Electric Circuits,* Addison-Wesley, London (1990).
20. F. G. Stremler, *Introduction to Communication Systems,* Addison-Wesley, London (1982).
21. M. S. Salisbury, P. F. McManamon, and B. D. Duncan, "Sensitivity improvement of a 1 μm ladar system incorporating an optical fiber preamp," *Opt. Eng.* **32(11),** 2671–2680 (Nov. 1993).
22. R. H. Barker, in *Communication Theory,* W. Jackson, Ed., Academic Press, London, (1953).

Leonard T. Masters received the Bachelor of Science degree in photonics from the State University of New York at Utica/Rome in 1993, and is currently pursuing the Master of Science degree in electro-optics at the University of Dayton. He has previously worked at Rome Labs at Griffiss Air Force Base, New York, evaluating and installing integrated optical modulators. He is currently performing ladar research for his degree at the Air Force Wright Laboratory, Wright-Patterson Air Force Base, Ohio.

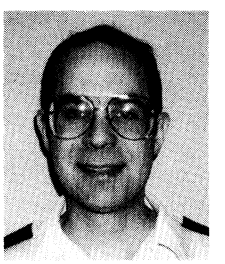

Martin B. Mark received his BS in electrical engineering from Purdue University in 1979, his MSEE from the Air Force Institute of Technology in 1980, and his PhD from Massachusetts Institute of Technology in 1986. He has been an officer in the U.S. Air Force since graduating from Purdue in 1979. In the Air Force, he has worked on the development of space-based optical communication systems, performed research involving numerous ladar systems, and taught electrical engineering at the U.S. Air Force Academy. He is currently performing ladar research at the Air Force Wright Laboratory, Wright-Patterson Air Force Base, Ohio.

Bradley D. Duncan: Biography and photograph appear with the special section guest editorial in this issue.